A&A 548, A15 (2012)
DOI: 10.1051/0004-6361/201219101

Astronomy & Astrophysics

From CoRoT 102899501 to the Sun⋆,⋆⋆,⋆⋆⋆

A time evolution model of chromospheric activity on the main sequence

P. Gondoin[1], D. Gandolfi[1,2], M. Fridlund[1], A. Frasca[3], E. W. Guenther[2], A. Hatzes[2], H. J. Deeg[4,5], H. Parviainen[4,5], P. Eigmüller[1,6], and M. Deleuil[7]

[1] European Space Agency, ESTEC – Postbus 299, 2200 AG Noordwijk, The Netherlands
e-mail: pgondoin@rssd.esa.int
[2] Thüringer Landessternwarte Tautenburg, Sternwarte 5, 07778 Tautenburg, Germany
[3] INAF – Osservatorio Astrofisico di Catania, via S. Sofia 78, 95123 Catania, Italy
[4] Instituto de Astrofísica de Canarias, 38205 La Laguna, Tenerife, Spain
[5] Departamento de Astrofísica, Universidad de La Laguna, 38206 La Laguna, Tenerife, Spain
[6] Institute of Planetary Research, German Aerospace Center, Rutherfordstrasse 2, 12489 Berlin, Germany
[7] Laboratoire d'Astrophysique de Marseille, 38 rue Frdric Joliot-Curie, 13388 Marseille Cedex 13, France

Received 23 February 2012 / Accepted 21 September 2012

ABSTRACT

Aims. The present study reports measurements of the rotation period of a young solar analogue, estimates of its surface coverage by photospheric starspots and of its chromospheric activity level, and derivations of its evolutionary status. Detailed observations of many young solar-type stars, such as the one reported in the present paper, provide insight into rotation and magnetic properties that may have prevailed on the Sun in its early evolution.

Methods. Using a model based on the rotational modulation of the visibility of active regions, we analysed the high-accuracy CoRoT lightcurve of the active star CoRoT 102899501. Spectroscopic follow-up observations were used to derive its fundamental parameters. We compared the chromospheric activity level of Corot 102899501 with the $R'_{\rm HK}$ index distribution vs age established on a large sample of solar-type dwarfs in open clusters. We also compared the chromospheric activity level of this young star with a model of chromospheric activity evolution established by combining relationships between the $R'_{\rm HK}$ index and the Rossby number with a recent model of stellar rotation evolution on the main sequence.

Results. We measure the spot coverage of the stellar surface as a function of time and find evidence for a tentative increase from 5−14% at the beginning of the observing run to 13−29% 35 days later. A high level of magnetic activity on Corot 102899501 is corroborated by a strong emission in the Balmer and Ca II H and K lines ($\log R'_{\rm HK} \sim -4$). The starspots used as tracers of the star rotation constrain the rotation period to 1.625 ± 0.002 days and do not show evidence for differential rotation.
The effective temperature ($T_{\rm eff} = 5180 \pm 80$ K), surface gravity ($\log g = 4.35 \pm 0.1$), and metallicity ([M/H] $= 0.05 \pm 0.07$ dex) indicate that the object is located near the evolutionary track of a $1.09 \pm 0.12\ M_\odot$ pre-main sequence star at an age of 23 ± 10 Myr. This value is consistent with the "gyro-age" of about 8−25 Myr, inferred using a parameterization of the stellar rotation period as a function of colour index and time established for the I-sequence of stars in stellar clusters.

Conclusions. We conclude that the high magnetic activity level and fast rotation of CoRoT 102899501 are manifestations of its stellar youth consistent with its estimated evolutionary status and with the detection of a strong Li I λ6707.8 Å absorption line in its spectrum. We argue that a magnetic activity level comparable to that observed on CoRot 102899501 could have been present on the Sun at the time of planet formation.

Key words. stars: activity – stars: atmospheres – stars: late-type – stars: magnetic field – stars: rotation – starspots

1. Introduction

Cool stars generate magnetic fields through dynamo processes in their interiors. These fields reach the stellar photospheres, where they produce cool spots. Magnetic fields also control outer stellar atmospheres. They heat stellar coronae and produce flares whose by-products, such as shock waves and high-energy particles, interact with the atmospheres of planets. One major topic in studying stellar activity is to explain how these magnetic phenomena seen on the Sun and stars depend on stellar parameters and their evolution.

Recent space-borne photometric missions such as CoRoT and *Kepler* provide precision photometry for a large number of stars with different stellar properties and ages, making these lightcurves a powerful tool for understanding stellar magnetic

⋆ Based on observations obtained with CoRoT, a space project operated by the French Space Agency, CNES, with participation of the Science Programme of ESA, ESTEC/RSSD, Austria, Belgium, Brazil, Germany and Spain.

⋆⋆ Based on observations made with the Anglo-Australian Telescope; the 2.1-m *Otto Struve* telescope at McDonald Observatory, Texas, USA; the Nordic Optical Telescope, operated on the island of La Palma jointly by Denmark, Finland, Iceland, Norway, and Sweden, in the Spanish Observatorio del Roque de los Muchachos of the Instituto de Astrofisica de Canarias, in time allocated by the NOT "Fast-Track" Service Programme, OPTICON, and the Spanish Time Allocation Committee (CAT).

⋆⋆⋆ The research leading to these results has received funding from the European Community's Seventh Framework Programme (FP7/2007-2013) under grant agreement number RG226604 (OPTICON).

Table 1. CoRoT, 2MASS, and USNO-A2 identifiers of the target star.

Main identifiers		
CoRoT ID	102899501	
2MASS ID	06483081-0234206	
USNO-A2 ID	0825-03232995	
Coordinates		
RA (J2000)	$06^h48^m30\overset{s}{.}81$	
Dec (J2000)	$-02°34'20\overset{''}{.}53$	
Magnitudes		
Filter	Mag	Error
B	13.727	0.047
V	12.846	0.056
r'	12.512	0.056
i'	11.934	0.065
J	11.095	0.026
H	10.570	0.022
Ks	10.461	0.021

Notes. Equatorial coordinates, optical, and near-infrared photometry are from the ExoDat catalogue (Deleuil et al. 2009) and 2MASS catalogue (Cutri et al. 2003).

activity. Although detailed analysis of only a small fraction of these lightcurves has been published, it has provided new information on rotation and differential rotation (Lanza et al. 2009; Fröhlich et al. 2009) as well as on the properties of spots (Silva-Valio et al. 2010), such as location, areal coverage, and lifetime (Mosser et al. 2009), for stars with different activity levels.

Part of the interest in magnetic phenomena comes from their possible impact on planet formation during the early phase of stellar evolution (Güdel 2007). One question in particular concerns the level of magnetic activity on the Sun in its infancy, when planets and their atmospheres formed. Detailed observations of many young solar-type stars, such as the one reported in the present paper, will provide insight into the rotation and magnetic properties that may have prevailed on the Sun at the beginning of the solar system history (Gaidos et al. 2000).

In this study, we report on the analysis of the high-accuracy lightcurve of the active star CoRoT 102899501, observed with the CoRoT satellite during its initial run in the exoplanet field IRa01 (Sect. 2.1). Its lightcurve exhibits spot-induced variability with a large amplitude and a short period that are indicative of high magnetic activity level coupled to rapid stellar rotation. These indicators are signs of stellar youth (Simon et al. 1985; Güdel et al. 1997; Soderblom et al. 2001), since rotation and magnetic activity on single late-type dwarfs decrease with stellar evolution.

The evolutionary status of CoRoT 102899501 was derived from spectroscopic observations performed at the Anglo-Australian Observatory, McDonald Observatory, and Nordic Optical Telescope (Sect. 2.2). The lightcurve analysis uses a model (Lanza et al. 2006) based on the rotational modulation of the visibility of active regions (Sects. 3.1 and 3.2). Chromospheric activity levels and lithium abundance were assessed using a spectral subtraction technique (Sects. 3.3 and 3.4). Results are discussed in Sect. 4.

2. Observations

2.1. CoRoT photometry

CoRoT 102899501 was photometrically observed with the space telescope CoRoT (Baglin et al. 2006; Auvergne et al. 2009) during the initial run IRa01, from 6 February to 2 April 2007. The lightcurve is continuous over 54 days with a sampling time of 512 s along the entire observation. The passband of the photometric data used in the present study ranges from 350 to 1000 nm. Identifiers of the target are reported in Table 1, along with its equatorial coordinates, optical and near-infrared magnitudes, as retrieved from the *ExoDat* database (Deleuil et al. 2009) and 2MASS catalogue (Cutri et al. 2003).

The pipeline reductions of the CoRoT lightcurve followed the scheme outlined by Barge et al. (2008). To detect and eliminate remaining outliers, we subtracted a moving-median filtered version of the reference lightcurve and flagged the points at distances greater than three times the dispersion of the residuals. These points were replaced by the median of previous and subsequent non-flagged values. Following the approach of Lanza et al. (2009), we computed a filtered version of the lightcurve by means of a sliding median boxcar filter with a boxcar extension approximately equal to one orbital period of the satellite, i.e. 6184 s (cf. Auvergne et al. 2009). This filtered lightcurve was subtracted from the original lightcurve, and all the points deviating more than three standard deviations of the residuals were discarded. Finally, we computed normal points by binning the data on time intervals having approximately the duration of the orbital period of the satellite, obtaining a lightcurve consisting of 752 points that cover 54 days (see Fig. 2). Each normal point was acquired by averaging 12 observations with a 512 s sampling.

We used the method described in Deeg et al. (2009) to quantify the straylight contamination from stars located in the vicinity of CoRoT 102899501. With the use of $BVr'i'$ images collected with the Wide Field Camera at the *Isaac Newton* Telescope (Deleuil et al. 2009), a reproduction of the CoRoT point spread function was folded over the positions of CoRoT 102899501 and neighbour stars while accounting for their brightness. We found that the light contamination factor is negligible, being less than 0.1%.

2.2. Groundbased follow-up spectroscopy

A reconnaissance low-resolution ($R \approx 1300$) spectrum of CoRoT 102899501 was acquired with the AAOmega multi-object facility (Sharp et al. 2006) at the Anglo-Australian Observatory in January 2009, as a part of the project devoted to study the stellar populations in the CoRoT exoplanet fields (Sebastian et al. 2012; Günther et al. 2012). Spectral type and luminosity class of the target star were derived by comparing the observed AAOmega spectrum with a grid of suitable templates, as described in Frasca et al. (2003) and Gandolfi et al. (2008). We found that CoRoT 102899501 is a K0 V star.

Figure 1 shows the best-fitting template (thick line) superimposed on the AAOmega spectrum of CoRoT 102899501 (thin line) for three spectral regions encompassing different lines: the Ca II H and K, Hδ and Hγ lines (upper left-hand panel), the Hβ line and Mg I triplet (upper right-hand panel), and the Hα and Li I 6708 Å lines (lower panel). A clear emission in both the Balmer and Ca II H and K lines is detected, confirming the high magnetic activity level suggested by the large amplitude of the CoRoT lightcurve. A deep Li I λ 6707.8 Å absorption line, well resolved from the nearby Ca I λ 6718 Å line, is also visible in the spectrum. By subtracting the best-fitting template from the observed spectrum, we estimated that the equivalent width (EW) of the Li I λ 6707.8 Å is ~300 mÅ.

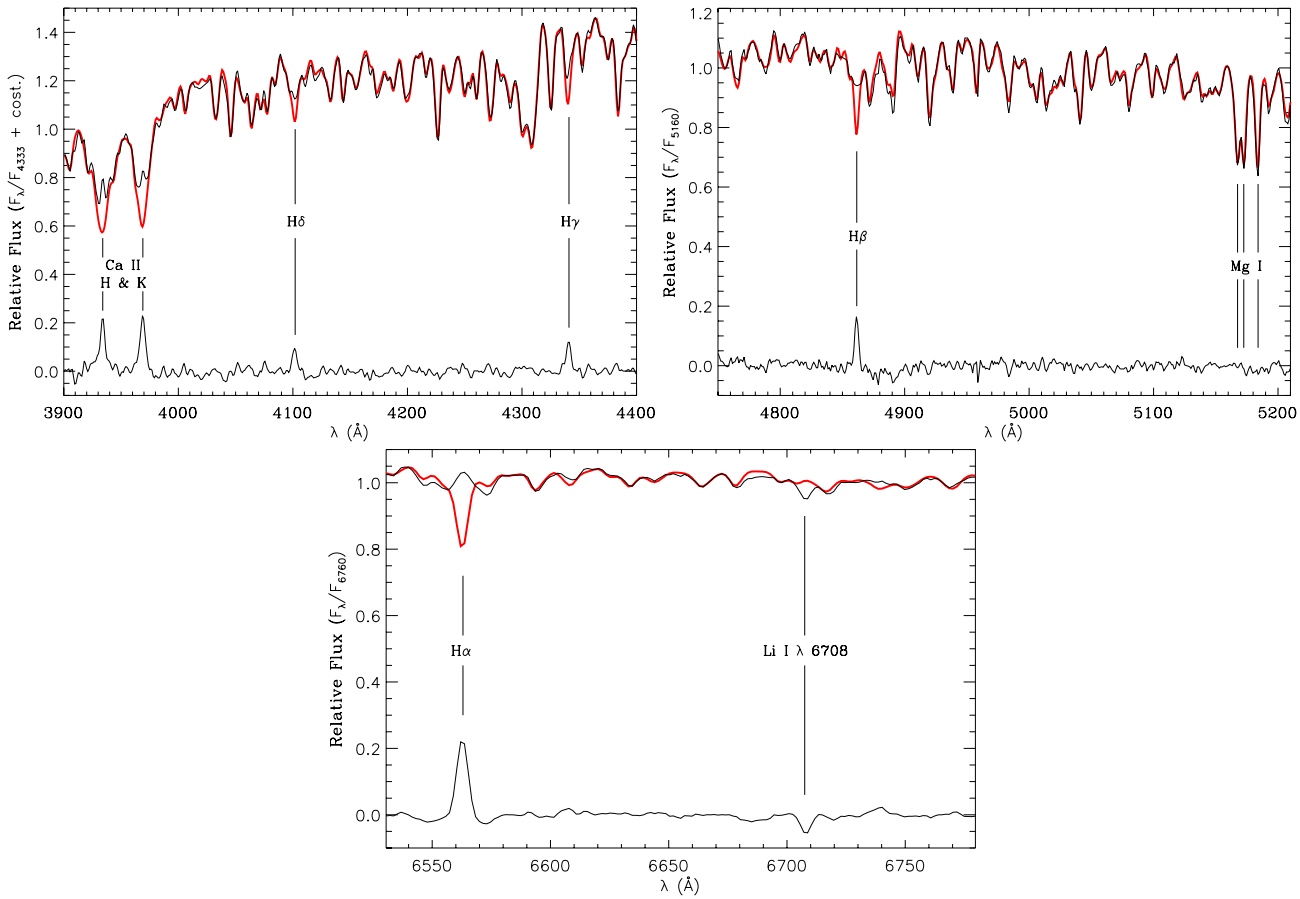

Fig. 1. AAOmega spectrum of CoRoT 102899501 (thin line) in three different spectral regions, along with the best-fitting template overplotted (thick line). The spectra have been arbitrarily normalised to the flux reported in the title of the vertical axis. The differences between observed and best-fitting spectrum are displayed in the lower part of each panel. Emission in the Balmer and Ca II H and K lines is detected, as well as a strong Li I λ 6707.8 Å absorption line, suggesting a young and active solar-like star.

Table 2. Radial velocities of CoRoT 102899501 as obtained with FIES and Sandiford spectrographs.

Date (UT) (yyyy/mm/dd)	HJD (days)	RV (km s^{-1})	σ_{RV} (km s^{-1})	S/N per pixel at 5500 Å	Instrument
2010/10/10	2 455 479.68731698	22.013	0.252	55	FIES
2010/10/28	2 455 497.65239003	21.460	0.350	13	FIES
2010/11/01	2 455 501.71001866	21.496	0.260	32	FIES
2011/01/19	2 455 581.38369968	21.516	0.297	22	FIES
2011/01/23	2 455 584.83710008	21.655	0.330	26	Sandiford
2011/01/24	2 455 585.87036894	21.598	0.356	16	Sandiford
2011/01/28	2 455 589.67732107	21.795	0.322	27	Sandiford
2011/01/29	2 455 590.72633521	21.250	0.342	28	Sandiford

Measurements of the star's radial velocity (RV) were performed to determine whether this rapidly rotating object is a single star or a member of a close binary system with tidally locked components. To this aim, we acquired four high-resolution spectra with the FIES fibre-fed echelle spectrograph (Frandsen & Lindberg 1999) attached to the 2.56 m Nordic Optical Telescope in La Palma (Spain) in October 2010 and January 2011, under the observing programs P40-418 and P42-216. The *Med-Res* fibre was used, yielding a resolving power of R = 47 800 in the spectral range 3700−7300 Å. We also acquired FIES template spectra of non-active, lithium-poor stars with the same spectral type as CoRoT 102899501 in December 2011 and January 2012, under observing programs P44-117 and P44-206, to determine the chromospheric activity level and photospheric lithium abundance of the target star (see Sects. 3.3 and 3.4). In January 2011 we gathered four additional high-resolution spectra with the Sandiford cass-echelle spectrometer (McCarthy et al. 1993), mounted at the 2.1 m (82 inch) *Otto Struve* Telescope of McDonald Observatory, Texas (USA). The spectra cover the wavelength range 5000−6000 Å with a resolving power of R = 47 000. Long-exposed ThAr spectra were acquired right before and after each FIES and Sandiford science spectrum to account for RV shifts of the instruments. The data were reduced using IRAF standard routines. We obtained RV measurements by cross-correlating the extracted science data with the spectrum of the radial velocity standard star HD 50692 (Udry et al. 1999), observed with the same instrument set-up.

Table 3. Stellar parameters of CoRoT 102899501 derived from the AAOmega, FIES, and Sandiford spectra.

Spectroscopic parameters	
$T_{\rm eff}$	5180 ± 80 K
$\log g$	4.35 ± 0.10
[Fe/H]	0.05 ± 0.07
$v \sin i$	36.0 ± 1.0 km s^{-1}
Sp.T.	K0 V

The FIES and Sandiford spectra reveal a single-peaked cross-correlation function with a relatively broad full-width at half maximum $FWHM = 62$ km s^{-1}, corresponding to a projected rotational velocity ($v \sin i$) of about 35 km s^{-1}. This is in agreement with the rapid rotation inferred from the CoRoT lightcurve and excludes a pole-on view of the star. If CoRoT 102899501 were a tidally locked binary system in a short period orbit ($P = 1.65$ days), its orbital angular momentum vector would be aligned with the stars' rotation spin axis. The system would thus be expected to have a variable RV component along the line of sight with an amplitude of several km s^{-1}. Although the accuracy of the RV measurements of CoRoT 102899501 is affected by the high rotation rate of the star, such a variable RV component is not detected (Table 2). This excludes the presence of a short-period stellar companion to CoRoT 102899501 with a high confidence level.

We used the co-added FIES and Sandiford spectra to derive effective temperature ($T_{\rm eff}$), surface gravity ($\log g$), metallicity ([M/H]), and projected rotational velocity ($v \sin i$) of CoRoT 102899501. Following the procedure usually adopted in CoRoT exoplanets' discovery papers (e.g. Fridlund et al. 2010; Gandolfi et al. 2010), we compared the co-added FIES and Sandiford spectra with a grid of synthetic model spectra from Castelli & Kurucz (2004); Coelho et al. (2005), and Gustafsson et al. (2008). We also employed the spectral analysis packages SME 2.1 (Valenti & Piskunov 1996; Valenti & Fischer 2005), as well as a modified version of the ROTFIT code (Frasca et al. 2003), which compares observed data with a set of template spectra of real stars with well-known parameters. Consistent results were obtained, regardless of the spectrum and method used. The final adopted values are $T_{\rm eff} = 5180 \pm 80$ K, $\log g = 4.35 \pm 0.10$ dex (CGS), [M/H] $= 0.05 \pm 0.07$ dex, and $v \sin i = 36 \pm 1$ km s^{-1} (Table 3), in agreement with the spectral type determination obtained from the AAOmega spectrum.

3. Data analysis

3.1. Stellar variability model

The rotation modulation of stellar photometric lightcurves by stellar active regions can be modelled using two numerical approaches: surface integration methods and the analytical method (Ribarik et al. 2003). The former assigns a temperature to each pixel of the spherical integration net and then varies each value until an optimal fit to the data is achieved. In the present study, we used the analytical approach described by Lanza et al. (2006), which is based on a model used to fit the time variations of the solar bolometric and spectral irradiance. Spots and faculae are modelled as point-like sources with flux contributions that account for their area and contrast. Although maximum-entropy regularised spot models show the best agreement with solar observations (Lanza et al. 2007), discrete spot models constrain spot longitudes and, as a consequence, the differential rotation. Following these models, the variation of the monochromatic stellar flux due to discrete active regions is given by

$$\Delta F(\lambda, t) = \Sigma_k \, \mu_k \, A_k \, I(\lambda, \mu_k) \;\; c_s(\lambda), \tag{1}$$

where $\Delta F(\lambda, t)$ is the perturbed stellar flux at wavelength λ and time t, and $\mu_k = \cos\psi_k$, with ψ_k the angle between the normal to the kth active region and the line of sight. A_k is the area of the cool spots in the kth active region. $I(\lambda, \mu_k)$ is the specific intensity of the unperturbed photosphere (which depends on μ owing to limb darkening), and c_s is the contrast of the cool spots (see Eq. (4)). Because of our ignorance of the structure of stellar active regions, the facular contribution was neglected based on the analysis results of the lightcurves of active dwarfs (Gondoin 2008). The summation in Eq. (1) is extended over the active regions on the visible hemisphere, i.e. for which $\mu_k > 0$. The value of μ_k is a function of time that is given by

$$\mu_k = \cos i \;\; \sin\theta_k \;\; + \;\; \sin i \;\; \cos\theta_k \;\; \cos(\Omega_k \, t + \Lambda_k), \tag{2}$$

where i is the inclination of the stellar rotation axis along the line of sight, θ_k is the latitude, Λ_k the longitude, and $\Omega_k = 2\pi/P_k$ the angular velocity of the kth active region having a rotation period P_k. The specific intensity of the undisturbed photosphere is

$$I(\lambda, \mu_k) = \frac{4 \, (a_{\rm p} + b_{\rm p} \, \mu + c_{\rm p} \, \mu^2)}{a_{\rm p} + 2b_{\rm p}/3 + c_{\rm p}/2} \; B(\lambda, T_{\rm eff}), \tag{3}$$

where the $a_{\rm p}$, $b_{\rm p}$, and $c_{\rm p}$ are the quadratic limb-darkening coefficients. Stellar oscillations are not taken into account in the lightcurve simulations that focus on a low-frequency domain of stellar variability. The effects of super-granulation, meso-granulation, and granulation are also neglected. The coefficients of the quadratic limb-darkening law adopted to describe the unperturbed bolometric specific intensity of the stars were derived from Claret (2000). The contrasts of the cool spots are assumed to be independent of their position on the stellar disk and are estimated as

$$c_s(\lambda) = \frac{B(\lambda, T_{\rm s})}{B(\lambda, T_{\rm eff})} - 1, \tag{4}$$

where $B(\lambda, T)$ is the Planck function, $T_{\rm s}$ is the spot effective temperature, and $T_{\rm eff}$ is the effective temperature of the unperturbed photosphere. The temperatures of starspots estimated using the Doppler imaging technique (e.g. Strassmeier et al. 2003) or from the variation of colour indexes vs rotation (e.g. Eaton 1992) are between 600 and 1600 K cooler than the unperturbed photosphere for most active stars. Berdyugina (2005) showed that, on average, this temperature difference appears larger for hotter stars, with values near 2000 K for the late F and early G stars dropping to 200 K for the late M stars (Strassmeier 2009). A value $T_{\rm s} - T_{\rm eff} \approx 1500$ K is found when $T_{\rm eff} = 5300$ K. In the model, we assumed $T_{\rm s} = 3800$ K .

The rotation period found by Fourier analysis is $P_{\rm rot} = 1.62 \pm 0.05$ days in agreement with Debosscher et al. (2009), with the uncertainty limited by the finite time duration of the lightcurve. Since starspots are used as tracers of the star rotation and can migrate in longitude, this value was refined by modelling the lightcurve itself with a three-spot model (see Sect. 3.2).

3.2. Lightcurve analysis

The relative flux variations of the sample star CoRoT 102899501 were fitted with the three-spot model described above. Best-fit models to the lightcurve were obtained by minimizing the sum

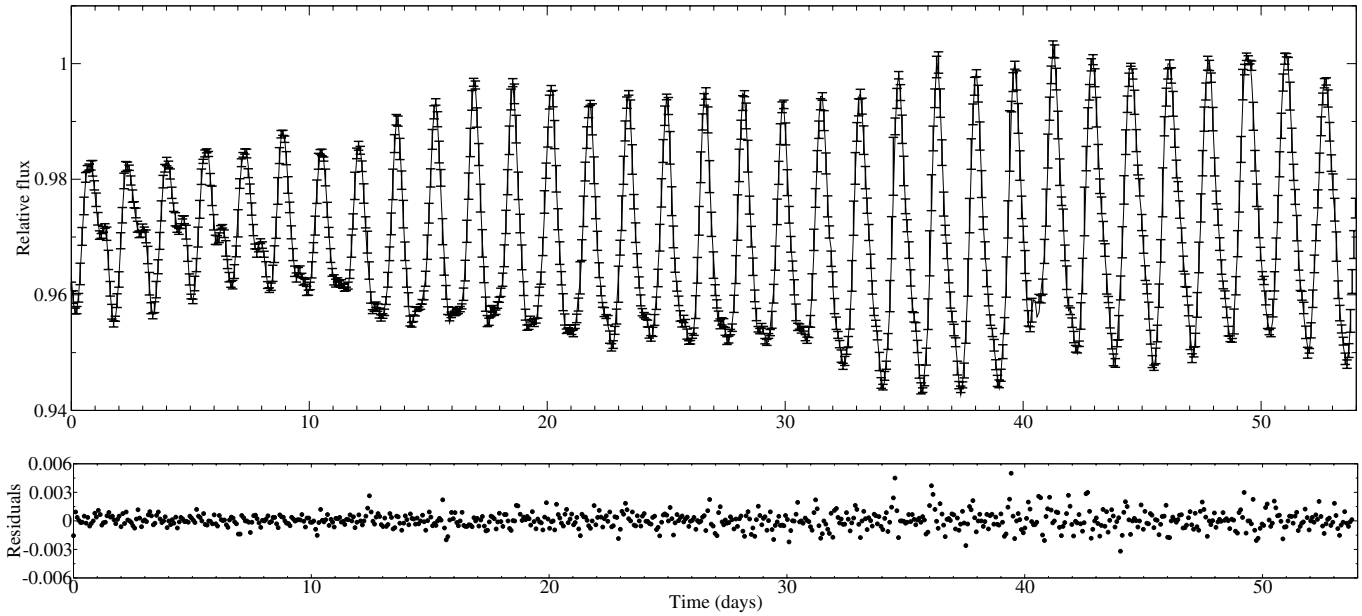

Fig. 2. Best-fit model (χ^2 = 0.90 for 407 degrees of freedom) to the lightcurve of CoRoT 102899501. The residuals to the best fit are shown in the lower panel.

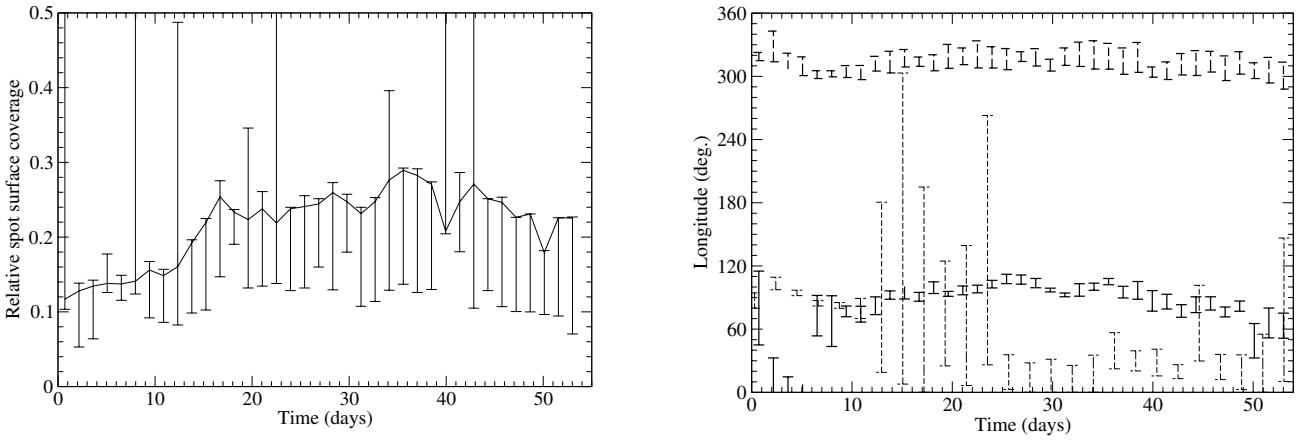

Fig. 3. Time evolution of the total spot surface coverage (*left*) and active longitude (*right*) on CoRoT 102899501 derived from its lightcurve analysis using a three-spot model. The three sets of symbols on the right-hand side correspond to the three spots used in the model.

Table 4. CoRoT 102899501 parameters used in the lightcurve analysis.

Model parameters		
Limb darkening	a_p	0.2005
Limb darkening	b_p	0.9905
Limb darkening	c_p	−0.1910
Rotation period	P_{rot} (d)	1.62
Spot temperature	T_s (K)	3800
Ratio of faculae to spots area	Q	0
Fitting time	$\Delta\, t_f$ (d)	1.45

Notes. The limb-darkening parameters were derived from Claret (2000) using a quadratic limb-darkening law for an LTE stellar model with effective temperature and gravity derived from the spectral analysis.

of squared residuals. The fixed parameters in the simulations included the stellar and active region parameters previously described. The surfaces, longitudes, and latitudes of the active regions were left as free parameters. The analyses of the lightcurve were performed using a three-spot model and iterating on nine variable parameters.

It was possible to obtain a good fit of the irradiance changes only for a limited time interval Δt_f = 1.45 days, i.e. about 90% of CoRoT 102599801 rotation period. Hence, the lightcurve was divided in 37 equal intervals covering 54 days of the time series. Each individual sub-lightcurve of 1.45 days' duration was fitted with the three-spot model to derive within each time interval average spot surfaces, latitudes, and longitudes. This method enabled us to estimate the time evolution of each spot parameter along the 54-day duration of the CoRoT 102599801 lightcurve (see Fig. 3). Using the same approach for modelling the rotation modulation of the Sun over several years, Lanza et al. (2003) found that the longest time interval that can be modelled with three stable active regions is 14 days, i.e. about 50% of the Sun rotation period. This was the lifetime of the sunspot group dominating the solar irradiance variations. In the case of other active stars, the value of Δt_f is determined from the observations themselves, looking for the maximum data extension that allows for a

good fit. In the case of the active star CoRoT-Exo-2 (Lanza et al. 2009), the maximum time interval Δt_f that could be fitted with a three-spot model turned out to be 3.2 days, i.e. 70% of the star rotation period.

Many series of fitting processes varying the inclination of the star rotation axis were conducted in order to identify the inclination angle that minimizes the overall χ^2 and the fitting parameters, for which the difference in χ^2 becomes significant at more than 99.99% confidence level. From the fits performed with a range of inclination angles, we kept those that gave the best fits within a 99.99% confidence level, using them to estimate a range in the other parameters of interest, i.e. spot areas, latitudes, and longitudes. An inclination angle $i = 87^{+1}_{-13}$ degrees was found with this new method. The consistency between the derived inclination angle and the spectroscopically measured projected equatorial velocity is addressed in Sect. 4. This range of inclination angles leads to uncertainties in the determination of spot parameters.

By modelling the rotational modulation of the total solar irradiance with the same method, Lanza et al. (2007) noted that the only quantities that can be safely derived are the longitudinal distribution of the active regions and the variation of their total area, measured with respect to a reference value corresponding to a given value of the irradiance assumed to be that of the unperturbed star. The estimated time evolution of the total spot surface coverage and of the active longitude on the star during the 2007 CoRoT initial run are displayed in Fig. 3. The analysis results do not show a conclusive variation of the spots' surface coverage which, according to the model, is included between ∼5−14% at the beginning of the observing run and ∼13−29%, 35 days later.

For comparison, Doppler images of active stars have shown starspots with a size up to 20% of a hemisphere (Strassmeier 2009). High filling factors, up to 50% of the stellar disk, have been determined from modelling molecular bands observed in the spectra of spotted stars (O'Neal et al. 1996, 1998). In particular, for the young G1.5 dwarf EK Dra that has been used as a proxy for the young Sun, O'Neal et al. (2004) derived a spot temperature of about 3800 K and a filling factor varying between 25% and 40%.

Figure 3 (right-hand panel) indicates that the active regions on the star photosphere experience no significant drift in longitude. Conversion of the best linear fit to these time evolutions of the longitudes between days 15 and 53 into rotation periods give values of 1.6266 ± 0.0008, 1.6240 ± 0.0005, and 1.6262 ± 0.0009 days for each of the three spots, respectively. The uncertainties on these rotation periods provide no conclusive indication of differential rotation on the surface of the star.

3.3. CaII H and K and Balmer lines emission

We used the FIES spectra with the highest signal-to-noise ratios acquired on 10 October and 1 November 2010 to measure the emission in the cores of the Ca II H and K and in the Hα, Hβ, and Hϵ Balmer lines using the spectral subtraction technique (see, e.g. Herbig 1985; Frasca & Catalano 1994). The method consisted of subtracting a reference spectral template of a non-active star. This template was obtained by a rotational broadening of the observed spectrum of a slowly rotating star with the same spectral type as CoRoT 102899501, but exhibiting no sign of magnetic activity. The net equivalent widths (EW) of the Ca II H and K, Hα, Hβ, and Hϵ lines (see Table 5) were measured by integrating the residual emission profile in the subtracted spectra (see Figs. 4 and 5).

Table 5. Line equivalent widths and associated radiative losses.

Line	Date (yyyy/mm/dd)	EW (Å)	Flux (erg cm^{-2} s^{-1})
Hα	2010/10/10	0.872 ± 0.075	4.24×10^6
Hα	2010/11/01	1.376 ± 0.214	6.68×10^6
Hβ	2010/10/10	0.256 ± 0.087	1.43×10^6
Hβ	2010/11/01	0.387 ± 0.134	2.16×10^6
Hϵ	2010/10/10	0.226 ± 0.150	0.58×10^6
Ca II H	2010/10/10	0.772 ± 0.160	1.97×10^6
Ca II K	2010/10/10	0.930 ± 0.220	2.01×10^6

The Ca II H and K lines display strong and fairly broad emission cores (Fig. 4). A line reversal with a slight asymmetry is visible only for the K line. while the H line does not show such behaviour owing to its lower signal-to-noise ratio. The Hϵ emission is barely visible in the observed spectrum, but appears clearly after subtraction of the non-active template (Fig. 4). The peak intensity of the Ca II H and K lines is comparable to that observed in KIC 8429280, a very young K2 star recently studied by Frasca et al. (2011).

Figure 5 (top) shows that, on 10 October 2010, the Hβ line is partially filled in with emission, while the Hα line is completely filled in with emission (see Table 5). The spectrum acquired on 1 November 2010 suggests an even higher activity level, since the Hβ line is filled in and the Hα line exhibits an emission profile above the continuum. Similar behavior has been observed on the very young K2 active stars, KIC 8429280 and LQ Hya, whose Hα lines vary from filled in to weak emission profiles (e.g. Strassmeier et al. 1993; Frasca et al. 2008).

We evaluated the radiative losses associated with the line excess emission following the guidelines of Frasca et al. (2010), i.e. by multiplying the average EW by the continuum surface flux at the wavelength of the line. The latter was evaluated by means of the spectrophotometric atlas of Gunn & Stryker (1983) and the angular diameters calculated by applying the Barnes & Evans (1976) relation. The EW and fluxes of the chromospheric lines are reported in Table 5. The EW and emission flux of the Ca II K line of CoRoT 102899501 are comparable to those of chromospherically active binaries with similar rotation periods (Montes et al. 1996).

On the basis of the Hα and Hβ flux, we evaluated a Balmer decrement $F_{H\alpha}/F_{H\beta} \simeq 3.0$ in both FIES spectra. Values of the Balmer decrement in the range 1–2 are typical of optically thick emission by solar and stellar plages (e.g. Buzasi 1989; Chester 1991), while prominences seen off-limb give rise to values of ∼10, which are typical of an optically thin emission source. This suggests that the bulk of the chromospheric emission of CoRoT 102899501 originates from magnetic regions similar to solar plages and that prominences play a marginal role.

3.4. Lithium abundance

Using the FIES raw spectra, we measured a Li I λ 6707.8 Å absorption line EW of about 320 mÅ in good agreement with the value inferred from the AAOmega spectrum (Sect. 2.2). This value must be corrected for the contribution of the close Fe I λ 6707.4 Å line, which is blended with the lithium line of CoRoT 102899501 due to its large $v \sin i$. Adopting the empirical relation proposed by Soderblom et al. (1993), $\Delta EW_{\rm Li\,I}$(mÅ) = $20 \times (B-V)_0 - 3$, a corrected value of $EW_{\rm Li\,I} \simeq 305$ mÅ is found.

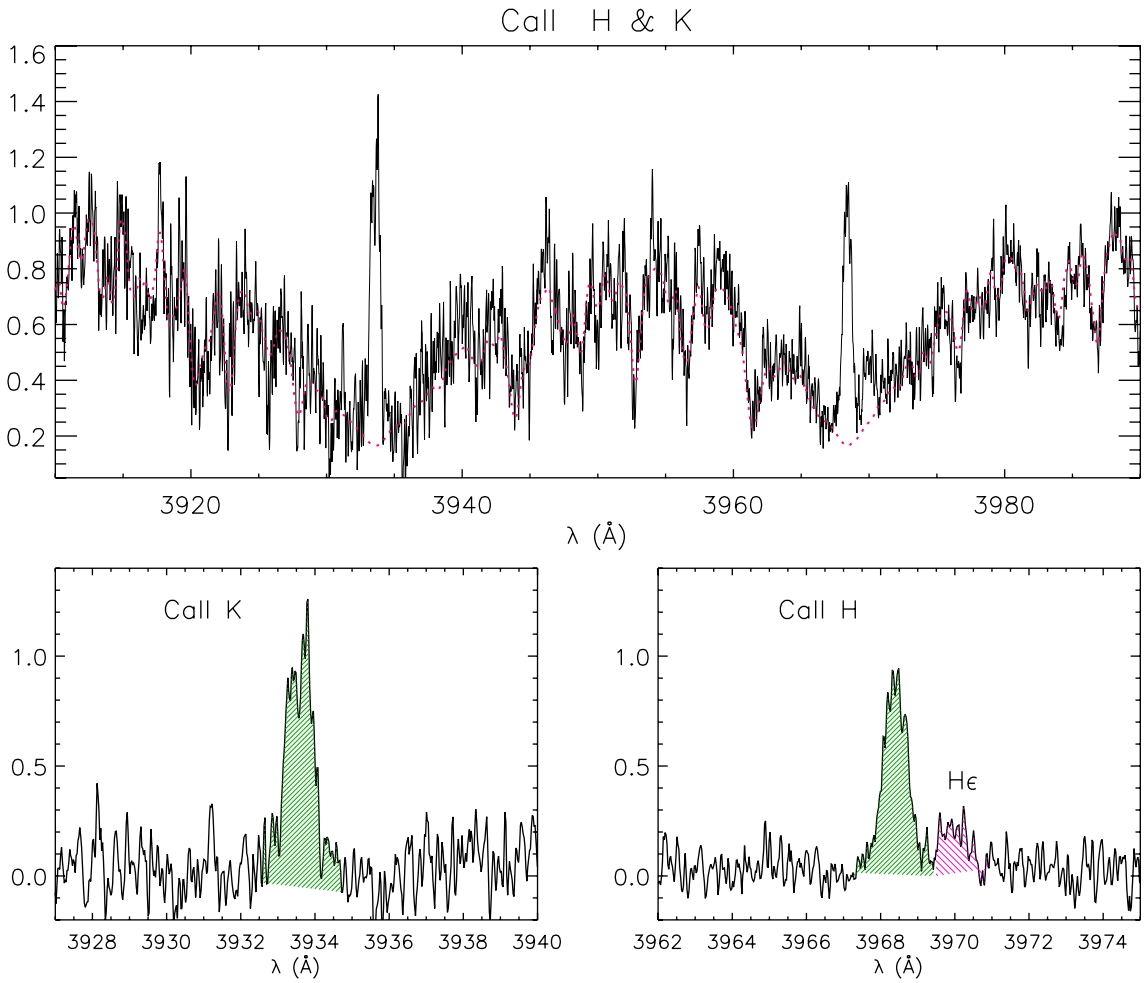

Fig. 4. *Top panel*: continuum-normalized spectrum of CoRoT 102899501 (solid line) in the Ca II H and K region observed on 2010 Oct. 10. The spectral template of the non-active star broadened at the $v \sin i$ of the target and Doppler-shifted according to the RV difference is overplotted with a dotted line. *Bottom panels*: difference spectrum where the Hϵ emission is emphasized.

We also measured the lithium EW on the difference spectrum obtained by subtracting a lithium-poor template broadened at the $v \sin i$ of CoRoT 102899501 and Doppler-shifted according to the RV difference. As shown in Fig. 6, all the photospheric lines, including the Fe I λ 6707.4 Å line, are removed in the subtraction, leaving as residuals a lithium absorption with $EW_{\rm Li\,I} = 295 \pm 50$ mÅ. Adopting the calibrations proposed by Pavlenko & Magazzù (1996), the lithium line EW translates into a high lithium abundance, $\log N(\mathrm{Li}) \simeq 3.15 \pm 0.25$.

4. Discussion

We analysed time-series photometric observations of the star CoRoT 102899501, observed with the CoRoT space telescope during the initial run IRa01 from 6 February to 2 April 2007. The lightcurve of the star shows an amplitude modulation up to almost 6% with a period of 1.625 days (see Fig. 2). Spectroscopic follow-up observations indicate that CoRoT 102899501 is a single K0 V star with $T_{\rm eff} = 5180 \pm 80$ K, $\log g = 4.35 \pm 0.10$, [M/H] = 0.05 ± 0.07 dex, and $v \sin i = 36 \pm 1$ km s^{-1} (Table 3). Emissions in both the Balmer line series and the Ca II H and K lines, as well as the presence of a strong Li I 6708 Å absorption line ($EW \approx 295 \pm 50$ mÅ) in the spectrum, suggest that the object is a young single star with a high level of magnetic activity. The bulk of the chromospheric emission of CoRoT 102899501 could be due to magnetic active regions similar to solar plages associated with sunspots.

Chromospheric activity has been traditionally measured using the $R'_{\rm HK}$ index, defined as the ratio of the emission in the core of Ca II H and K lines to the total bolometric emission of the star (Noyes et al. 1984). We derived a value $\log(R'_{\rm HK}) = -4.01^{+0.11}_{-0.14}$ for CoRoT 102899501, injecting the measured emission fluxes $F'_{\rm H}$ and $F'_{\rm K}$ in the cores of the Ca II H and K lines (see Table 5) into the following expression (Martinez-Arnaiz et al. 2010):

$$R'_{\rm HK} = \frac{F'_{\rm H} + F'_{\rm K}}{\sigma T_{\rm eff}^4}, \qquad (5)$$

where σ is the Stefan-Boltzmann constant. This value is similar to that of the most active solar-type dwarfs among a sample of main sequence and pre-main sequence stars compiled by Mamajek & Hillenbrand (2008). These authors show that a chromospheric activity index $\log(R'_{\rm HK}) \approx -4$ is found among solar-type dwarfs that are members of young stellar associations such as Upper Sco (age ~ 5 Myr), β Pic (~12 Myr), Upper Cen-Lup (~16 Myr) or Lower Cen Cru (~16 Myr). Sun-like stars that are members of older open clusters such as α Per (~85 Myr), the Pleiades (~130 Myr), UMa (~500 Myr), the Hyades (~625 Myr), or M 67 (~400 Myr) have significantly lower Ca II emissions (see Fig. 7).

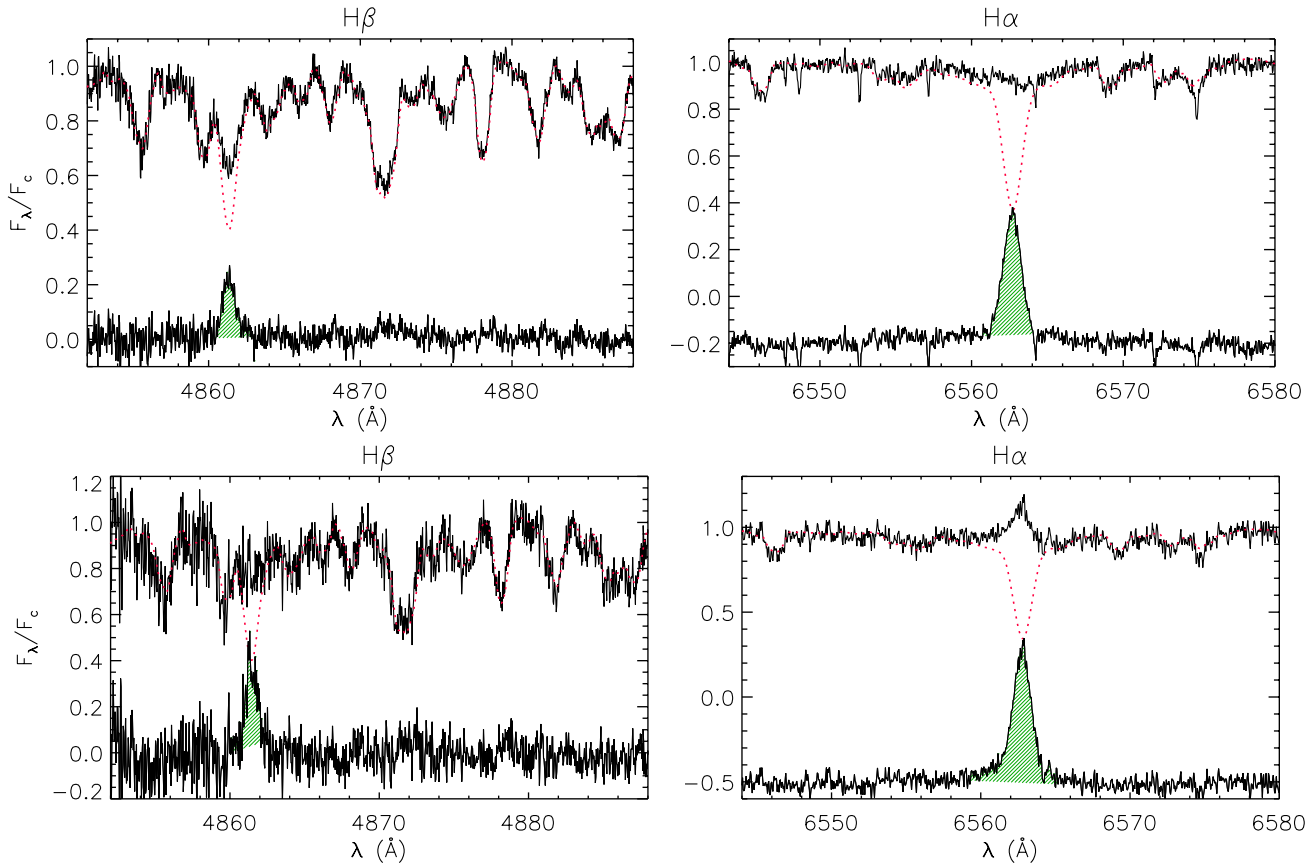

Fig. 5. *Top of each panel*: observed, continuum-normalized FIES spectra of CoRoT 102899501 (solid line) acquired on 2010 October 10 (*upper panels*) and 2010 November 1 (*lower panels*) in the Hβ (*left panels*) and Hα (*right panels*) regions. The spectrum template of the non-active star is represented in dotted lines. *Bottom of each panel*: difference between observed and template spectra. The residual Hα profile is shifted downwards for the sake of clarity. The hatched areas represent the excess emissions that have been integrated to obtain the net line EW.

We fitted the relative flux variations of the star's lightcurve with a three-spot model. Assuming a 3800 K spot temperature, the analysis result suggests a large coverage of CoRoT 102899501 photosphere by active regions. It does not show a conclusive variation of the spots' surface coverage, which, according to the model, is included between ∼5−14% at the beginning of the observing run and ∼13−29%, 35 days later. The starspots used as tracers of the star rotation constrain the rotation period to 1.625 ± 0.002 days and do not show evidence for differential rotation. CoRoT 102899501 is characterized by a high level of magnetic activity most likely linked to its fast rotation and spectral type.

The effective temperature, gravity, and metallicity derived from the spectroscopic observation of the target (Sect. 2.2) were compared with evolutionary models of stars with the same metal abundance. These models were computed by Siess et al. (2000) using the Grenoble stellar evolution code (Forestini 1994) and by Marques et al. (2008) using the CESAM code (Morel 1997; Morel & Lebreton 2008) and the initial condition of the birth line from Palla & Stahler (1991, 1992). The comparison shows that CoRoT 102899501 is located near the evolutionary tracks of a $1.09 \pm 0.12\ M_{\odot}$ pre-main sequence star at an age of 23 ± 10 Myr.

The comparison also indicates that the radius of the star is included between 0.96 $R_{\odot}$ and 1.36 $R_{\odot}$. Taking into account the rotation period ($P_{\rm rot} = 1.625 \pm 0.002$ days) and the inclination angle ($74° < i < 88°$) of the star, as derived from the analysis of its lightcurve, we found $v \sin i = 35.6 \pm 6.9$ km s^{-1}. The good agreement with the projected equatorial velocity $v \sin i = 36 \pm 1$ km s^{-1} inferred independently from the broadening of the spectral lines supports the consistency of the overall analysis.

A 1.625-day rotation period divided by a convective turnover time $\tau_c = 12.7$ days for a 1.09 $M_{\odot}$ main sequence star (Wright et al. 2011) leads to a Rossby number $R_0 = 0.13$. Applying the empirical relation between the $R'_{\rm HK}$ index and the Rossby number (see Eq. (7)) established by Mamajek & Hillenbrand (2008), one finds $R'_{\rm HK} = -4.08 \pm 0.03$ in good agreement with the measured emission fluxes in the core of the Ca II lines of CoRoT 102899501.

We followed the method described in Gandolfi et al. (2008) to derive the interstellar extinction towards CoRoT 102899501. Adopting a normal value for the ratio of total-to-selective extinction ($R_V = A_V/E_{B-V} = 3.1$), we found $A_V = 0.35 \pm 0.15$ mag and an absorption-corrected star V magnitude equal to 12.49 ± 0.21. A comparison with the absolute magnitude $M_V = 5.13 \pm 0.40$ inferred from the evolutionary models leads to a true distance modulus of 7.36 ± 0.61 that corresponds to a distance of 308 ± 85 pc.

Solar-type stars reach the zero-age main sequence (ZAMS) rotating at a variety of rates, as seen in the Pleiades (Stauffer & Hartmann 1987; Soderblom et al. 1993). However, it has been noted (see, e.g., Barnes 2003; Meibom et al. 2009) that these young stars tend to group into two main sub-populations that lie on narrow sequences in diagrams where the measured rotation periods of the members of a stellar cluster are plotted against their $B - V$ colours. One sequence, called the I sequence, consists of stars that form a diagonal band of increasing rotation period with increasing $B - V$ colour. In young clusters, another

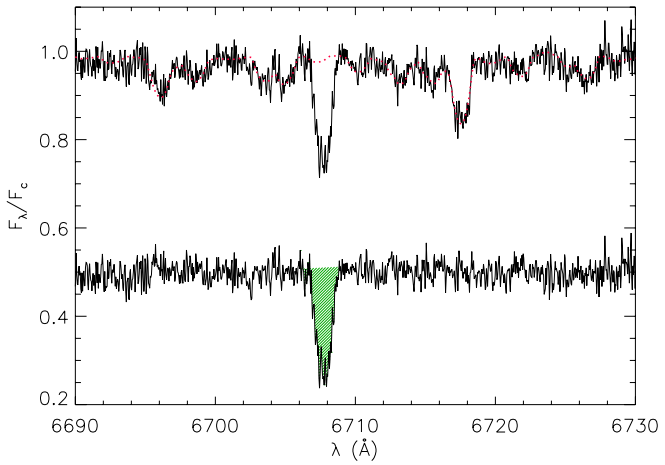

Fig. 6. Continuum-normalized FIES spectrum of CoRoT 102899501 obtained on 2010 October 1 in the lithium line region. The template spectrum of a lithium-poor reference star broadened at the $v \sin i$ of CoRoT 102899501 and Doppler-shifted according to the RV difference is shown in dotted line. The lithium absorption is cross-hatched in the difference spectrum whose continuum has been set arbitrarily at a 0.5 level.

sequence of ultra-fast rotating stars called the *C*-sequence, is also observed, bifurcating away from the *I*-sequence towards shorter rotation periods.

A parameterization of the stellar rotation period as a function of colour index and time is proposed by Barnes (2003) for the two sequences, thus opening the possibility of using stellar gyrochronology for "gyro-age" determination. Applying these relationships to CoRot 102899501 (P = 1.625 days; $(B-V)_0$ = 0.77 ± 0.15 mag), we found ages in the range 70−180 Myr and 8−25 Myr, using the *C*- and the *I*-sequence relationship, respectively. The age inferred from the *I*-sequence relationship is in good agreement with the 23 ± 10 Myr value derived from the stellar evolution models. According to the physical explanation of the *I*-sequence proposed by Barnes (2003), this suggests that the magnetic fields on CoRoT 102899501, which cause angular momentum loss by coupling the surface of the star to the magnetized wind, are also able to couple to a substantial fraction of the whole star, which could be essentially in solid body rotation.

The C/I dichotomy for stellar rotation was recently formulated mathematically by Barnes (2010) in a simple model that describes the rotational evolution of cool stars on the main sequence. According to this model, the time evolution of the rotational period of a main sequence star depends on two parameters, (i) its initial period of rotation P_0 on the ZAMS and (ii) its convective turnover time. These parameters are related by the following expression (Barnes 2010):

$$t = \frac{\tau_{c,B}}{k_C} \times \ln\left(\frac{P(t)}{P_0}\right) + \frac{k_I}{2\tau_{c,B}} \times \left(P(t)^2 - P_0^2\right), \quad (6)$$

where the constants k_c = 0.646 days Myr^{-1}, k_I = 452 Myr day^{-1}, and $\tau_{c,B}$ = 34.884 days have been calibrated on the Sun with input from open-cluster rotation observations, demanding that the rotation of the star starts off with an initial period of 1.1 days and be 26.09 days at the age of 4570 Myr (Barnes 2010). We combined the above expression with the unique mass-independent prediction of the chromospheric activity index R'_{HK} (Mamajek & Hillenbrand 2008), expressed as follows:

$$\log R'_{HK} = A - B \times \left(\frac{P(t)}{\tau_c} - C\right)$$
$$A, B, C = \begin{cases} -4.23, 1.451, 0.233 \text{if } P(t)/\tau_c < 0.32 \\ -4.522, 0.337, 0.814 \text{if } P(t)/\tau_c \geq 0.32. \end{cases} \quad (7)$$

The combination of Eqs. (6) and (7) constitutes a simple time evolution model of the chromospheric activity of main sequence stars as a function of the stars convective turnover time and initial period of rotation P_0 on the ZAMS. The dependence on mass of the R'_{HK} index is defined by the parameterization of the convective turnover time as a function of stellar mass provided by Wright et al. (2011):

$$\log(\tau_{c,W}) = 1.16 - 1.49 \times \log\left(\frac{M}{M_\odot}\right) - 0.54 \times \log^2\left(\frac{M}{M_\odot}\right). \quad (8)$$

In Eq. (6), we rescaled the turnover time mass dependence of Wright et al. (2011) by a factor $(\tau_{c,B}/\tau_{c,W})_\odot \approx 2.4$ to correct for the different value of the Sun convective turnover time used by Barnes (2010). Using the above model, we calculated the time evolution of the R'_{HK} index time of a Sun-like star with an initial period of rotation on the ZAMS and a mass identical to that of CoRoT 102899501. The results are compared with the median log (R'_{HK}) values of the Sun and of solar-type dwarfs in open stellar clusters with different ages compiled by Mamajek & Hillenbrand (2008). The comparison shows that the high level of chromospheric activity of the CoRoT 102899501 is linked with its fast rotation due to its young age.

In view of the low value of its Rossby number, CoRoT 102899501 is expected to emit X-rays in the saturation regime of coronal emission at an X-ray to bolometric luminosity ratio $L_X/L_{bol} \approx 10^{-3}$ (Pizzolato et al. 2003) corresponding to $L_X \approx 3 \times 10^{30}$ erg s^{-1}. It has been argued that the saturated regime of X-ray emission is associated with a turbulent dynamo (Wright et al. 2011) and that a dynamo regime transition, possibly between a turbulent dynamo and an interface-type dynamo, occurs at a Rossby number of 0.3 (Gondoin 2012). This could also explain the change in the log(R'_{HK}) vs. rotation relationship observed by Mamajek & Hillenbrand (2008) around this Rossby number value. CoRoT 102899501 and the Sun could thus be generating magnetic fields in different dynamo regimes.

A deep Li I λ6707.8 Å photospheric absorption line along with magnetic activity indicators as observed in the spectrum of CoRoT 102899501 are generally considered as a sign of stellar youth (e.g. Soderblom et al. 1998). Lithium is indeed expected to be strongly depleted from the stellar atmospheres of late-type stars when mixing mechanisms pull it deeply in their convective layers. It has thus been suggested (e.g. Skumanich 1972) that the lithium surface abundance should decrease with stellar evolution. Recently Da Silva et al. (2009) derived the distribution of lithium abundances in nine stellar associations covering ages from 5 Myr up to that of the Pleiades (100 Myr). These authors measured a systematic decrease of lithium abundance with age in the temperature range from about 3500 K to 5000 K. They concluded that the age sequence of the young associations based on the lithium abundance measurements agrees well with isochronal age determination. However, they also noticed a scatter of lithium abundance value that hampers the determination of reliable age on individual stars. Also, lithium depletion has been found in several T Tauri stars at levels inconsistent with their young ages (Magazzù et al. 1992; Martin et al. 1994).

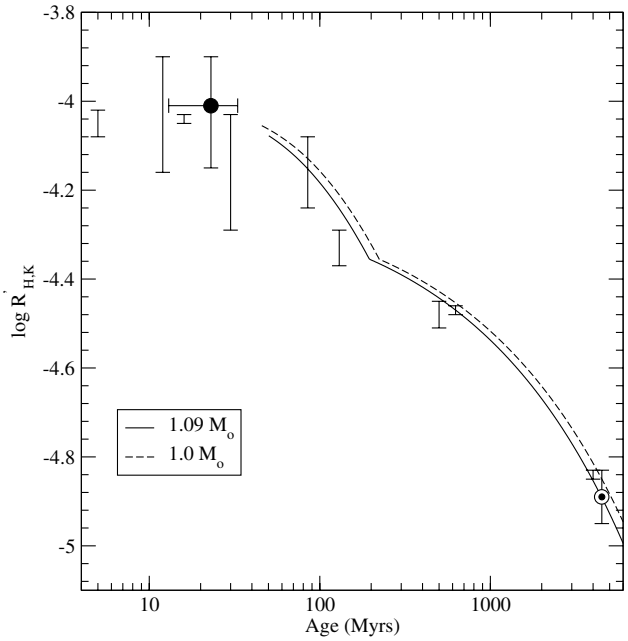

Fig. 7. Time evolution model of the chromospheric activity of Sun-like stars on the main sequence compared with the median chromospheric activity indices of the Sun and solar-type dwarfs in Upper Sco (age ∼ 5 Myr), β Pic (∼12 Myr), Upper Cen-Lup (∼16 Myr), Lower Cen Cru (∼16 Myr), α Per (∼85 Myr), the Pleiades (∼130 Myr), UMa (∼500 Myr), the Hyades (∼625 Myr), and M67 (∼4000 Myr) compiled by Mamajek & Hillenbrand (2008). The value of the chromospheric activity index log ($R'_{\rm HK}$)of CoRoT 102899501 is indicated with a black circle.

Although lithium cannot be used as a reliable age indicator for a single star, it is worth noting that the measured EW of the lithium line ($EW_{\rm Li\,I}$ = 0.295 ± 0.050 Å) in CoRoT 102899501 spectrum is larger than the upper envelopes of the lithium equivalent widths in the dwarf spectra of both the Pleiades (100 Myr; Soderblom et al. 1993) and α Per cluster (50 Myr; Sestito & Randich 2005). The CoRoT 102899501 $EW_{\rm Li\,I}$ value is actually comparable to that of stars with similar effective temperatures in the young cluster IC 2602 (30 Myr, Montes et al. 2001). This suggests an age ≤30 Myr consistent with the age determinations inferred from the gyrochronology method and from the comparison with stellar evolution models.

Our analysis of a large set of photometric and spectroscopic observations of CoRot 102899501 provides a consistent set of stellar parameters, activity level, and age for a single field star. In particular, the stellar evolution models, lithium abundance, and the gyrochronology technique concur with an age estimate in the range of 8−30 Myr. Moreover, the chromospheric activity of CoRot 102899501 is consistent with the $R'_{\rm HK}$ index measured on a sample of solar-like dwarfs in young open clusters. These chromospheric activity levels, together with those observed on solar-type dwarfs in older open clusters and on the Sun, are also in line with a model of chromospheric activity evolution on the main sequence that we established by combining $R'_{\rm HK}$ vs. Rossby number relationships with a recent model of stellar rotation evolution on the main sequence (Barnes 2010). We thus conclude that a magnetic activity level comparable to that observed on CoRot 102899501 could have been present on the Sun at the time of planets' formation.

Acknowledgements. We are grateful to Dr. A. Baglin and to the CoRoT team for the outstanding quality of the CoRoT data. A.H., D.G., and E.G. acknowledge the support of the grants 50OW0204 from the Deutschen Zentrums für Luft- und Raumfahrt (DLR). The team at the IAC acknowledges support by grant AYA2010-20982-C02-02 of the Spanish Ministry of Economy and Competitiveness. The authors are grateful to the staff at AAO, NOT, and McDonald Observatories for their valuable support and contribution to the success of the AAOmega, FIES, and Sandiford observing runs. We are grateful to the anonymous referee for the helpful comments that allowed us to improve the paper.

References

Auvergne, M., Bodin, P., Boisnard, L., et al. 2009, A&A, 506, 411
Baglin, A., Auvergne, M., Boisnard, L., et al. 2006, 36th COSPAR Scientific Assembly, 36, 3749
Barge, P., Baglin, A., Auvergne, M., et al. 2008, A&A, 482, L17
Barnes, S. A. 2003, ApJ, 586, 464
Barnes, S. A. 2010, ApJ, 722, 222
Barnes, T. G., & Evans, D. S. 1976, MNRAS, 174, 489
Berdyugina, S. V. 2005, Liv. Rev. Sol. Phys., 2, 8
Bouvier, J., Forestini, M., & Allain, S. 1997, A&A, 336, 1023
Buzasi, D. L. 1989, Ph.D. Thesis, Pennsylvania State Univ.
Castelli, F., & Kurucz, R. L. 2004 [arXiv:astro-ph/0405087]
Chester, M. M. 1991, Ph.D. Thesis, Pennsylvania State Univ.
Claret, A. 2000, A&A, 363, 1081
Coelho, P., Barbuy, B., Meléndez, J., et al. 2005, A&A, 443, 735
Cutri, R. M., Skrutskie, M. F., van Dyk, S., et al. 2003, 2MASS All-Sky Catalog of Point Sources, NASA/IPAC Infrared Science Archive
Da Silva, L., Torres, C. A. O., de la Reza, R., et al. 2009, A&A, 508, 833
Debosscher, J., Sarro, L. M., López, M., et al. 2009, A&A, 506, 519
Deeg, H. J., Gillon, M., Shporer, A., et al. 2009, A&A, 506, 343
Deleuil, M., Meunier, J. C., Moutou, C., et al. 2009, AJ, 138, 649
Eaton, J. A. 1992, LNP, 397, 15
Flower, P. J. 1996, ApJ, 469, 355
Forestini, M. 1994, A&A, 285, 473
Frandsen, S., & Lindberg, B. 1999, in Astrophysics with the NOT, eds. H. Karttunen & V. Piirola, 71
Frasca, A., & Catalano, S. 1994, A&A, 284, 883
Frasca, A., Alcalá, J. M., Covino, E., et al. 2003, A&A, 405, 149
Frasca, A., Kővári, Z. S., Strassmeier, K. G., & Biazzo, K. 2008, A&A, 481, 229
Frasca, A., Biazzo, K., Kővári, Z. S., Marilli, E., & Çakırlı, Ö. 2010, A&A, 518, A48
Frasca, A., Fröhlich, H.-E., Bonanno, A., et al. 2011, A&A, 532, A81
Fridlund, M., Hébrard, G., Alonso, R., et al. 2010, A&A, 512, A14
Fröhlich, H.-E., Küker, M., Hatzes, A. P., & Strassmeier, K. G. 2009, A&A, 506, 263
Gaidos, E. J., Henry, J. W., & Henry, S. M. 2000, AJ, 120, 1006
Gandolfi, D., Alcalá, J. M., Leccia, S., et al. 2008, ApJ, 687, 1303
Gandolfi, D., Hébrard, G., Alonso, R., et al. 2010, A&A, 524, A55
Gondoin, P. 2008, A&A, 478, 883
Gondoin, P. 2012, A&A, 546, A117
Güdel, M. 2007, Liv. Rev. Sol. Phys., 4, 3
Güdel, M., Guinan, E. F., & Skinner, S. L. 1997, ApJ, 483, 947
Gunn, J., & Stryker, L. L. 1983, ApJS, 52, 121
Günther, E. W., Gandolfi, D., Sebastian, D., et al. 2012, A&A, 543, A125
Gustafsson, B., Edvardsson, B., Eriksson, K., et al. 2008, A&A, 486, 951
Herbig, G. H. 1985, ApJ, 289, 269
Lanza, A. F., Rodonò, M., Pagano, I., et al. 2003, A&A, 403, 1135
Lanza, A. F., Messina, S., Pagano, I., & Rodonò, M. 2006, Astron. Nachr., 327, 21
Lanza, A. F., Bonomo, A. S., & Rodonò, M. 2007, A&A, 464, 741
Lanza, A. F., Pagano, I., Leto, G., et al. 2009, A&A, 493, 193
Lunine, J. I., O'Brien, D., P., Raymond, S. N., et al. 2009, Adv. Sci. Lett., Special Issue on Computational Astrophysics, ed. L. Mayer [arXiv:0906.4369]
Magazzù, A., Rebolo, R., & Pavlenko, I. V. 1992, ApJ, 392, 159
Mamajek, E. E., & Hillenbrand, L. A. 2008, ApJ, 687, 1264
Marques, J. P., Monteiro, M. J. P. F. G., & Fernandes, J. M. 2008, Ap&SS, 316, 173
Martin, E. L., Rebolo, R., Magazzu, A., & Pavlenko, Y. V. 1994, A&A, 282, 503
Martínez-Arnáiz, R., Maldonado, J., Montes, D., Eiroa, C., & Montesinos, B. 2010, A&A, 520, A79
McCarthy, J. K., Sandiford, B. A., Boyd, D., & Booth J. 1993, PASP, 105, 881
Meibom, S., Mathieu, R. D., & Stassun, K. G. 2009, AJ, 695, 679
Montes, D., Fernández-Figueroa, M. J., Cornide, M, & De Castro, E. 1996, A&A, 312, 221

Montes, D., López-Santiago, J., Fernández-Figueroa, M. J., & Gálvez, M. C. 2001, A&A, 379, 976
Morel, P. 1997, A&AS, 124, 597
Morel, P., & Lebreton, Y. 2008, Ap&SS, 316, 61
Mosser, B., Baudin, F., Lanza, A. F., et al. 2009, A&A, 506, 245
Noyes, R. W., Hartmann, L. W., Baliunas, S. L., et al. 1984, ApJ, 279, 763
O'Neal, D., Saar, S. H., & Neff, E. 1996, ApJ, 463, 766
O'Neal, D., Saar, S. H., & Neff, E. 1998, ApJ, 507, 919
O'Neal, D., Neff, J. E., Saar, S. H., & Cuntz, M. 2004, AJ, 128, 1802
Palla, F., & Stahler, S. W. 1991, ApJ, 375, 288
Palla, F., & Stahler, S. W. 1992, ApJ, 392, 667
Pavlenko, Y. V., & Magazzù, A. 1996, A&A, 311, 961
Pizzolato, N., Maggio, A., Micela, G., Sciortino, S., & Ventura, P. 2003, A&A, 397, 147
Ribarik, G., Olah, K., & Strassmeier, K. G. 2003, Astron. Nachr., 324, 202
Sebastian, D., Guenther, E. W., Schaffenroth, V., et al. 2012, A&A, 541, A34
Sestito, P., & Randich, S. 2005, A&A, 442, 615
Sharp, R., Saunders, W., Smith, G., et al. 2006, SPIE, 6269
Siess, L., Dufour, E., & Forestini, M. 2000, A&A, 358, 593
Silva-Valio, A., Lanza, A. F., Alonso, R., & Barge, P. 2010, A&A, 510, A25
Simon, T., Herbig, G., Boesgaard, et al. 1985, ApJ, 293, 551
Skumanich, A. 1972, ApJ, 171, 565
Soderblom, D. R., Jones, B. F., Balachandran, S., et al. 1993, AJ, 106, 1059
Soderblom, D. R., King, J. R., & Henry, T. J. 1998, AJ, 116, 396
Soderblom, D. R., Jones, B. F., & Fischer, D. 2001, ApJ, 563, 334
Stauffer, J. R., & Hartmann, L. W. 1987, ApJ, 318, 337
Strassmeier, K. G. 2009, A&A Rev., 17, 251
Strassmeier, K. G., Rice, J. B., Wehlau, W. H., Hill, G. M., & Matthews, J. M. 1993, A&A, 268, 671
Strassmeier, K. G., Pichler, T., Weber, M., & Granzer, T. 2003, A&A, 411, 595
Telleschi, A., Güdel, M., Briggs, K., et al. 2005, ApJ, 622, 653
Valenti, J. A., & Piskunov, N. 1996, A&AS, 118, 595
Valenti, J. A., & Fischer, D. A. 2005, ApJS, 159, 141
Udry, S., Mayor, M., & Queloz, D. 1999, in Precise Stellar Radial Velocities, eds. J. B. Hearnshaw, & C. D. Scarfe, IAU Colloq., 170, ASP Conf. Ser., 185, 367
Wright, N. J., Drake, J. J., Mamajek, E. E., & Henry, G. W. 2011, ApJ, 743, 48